

Effect of electrolyte composition on micro-arc anodization of AM60B magnesium alloy

M. Bestetti, F. Barlassina, A. Da Forno, P.L. Cavallotti

Politecnico di Milano - Dipartimento di Chimica, Materiali e Ingegneria Chimica "G. Natta" - Milano (Italia)

ABSTRACT

Anodic oxidation in micro-arc regime is one of the most investigated techniques used to coat magnesium alloys with ceramic coatings for protection from corrosion and wear. The anodization electrolyte composition affects the current/voltage characteristic of the cell, the anodic oxide layer morphology and its behaviour in aggressive environment. In this paper the influence of the electrolyte composition on the anodic oxidation process and oxide properties is discussed. Scanning electron microscopy, x-ray diffraction, and x-ray photoelectron spectroscopy were employed to assess morphology, crystallographic structure and composition of the anodic oxide. Electrochemical polarization tests were performed to evaluate the corrosion resistance behaviour of the coated magnesium alloys.

RIASSUNTO

L'ossidazione anodica in regime di micro-arco è una delle tecniche maggiormente studiate tra quelle utilizzate per proteggere le leghe di magnesio da corrosione e usura con rivestimenti ceramici. La composizione del bagno elettrolitico di anodizzazione influenza le curve caratteristiche corrente /voltaggio, la morfologia dello strato di ossido anodico e il suo comportamento in ambiente aggressivo. In questo articolo si descrive l'influenza della composizione del bagno elettrolitico sul processo di ossidazione anodica e sulle proprietà dell'ossido. Microscopia a scansione elettronica, diffrazione di raggi X, spettroscopia fotoelettronica indotta da raggi X sono utilizzate per valutare la morfologia, la struttura cristallografica e la composizione dell'ossido anodico. Prove di polarizzazione elettrochimica sono state effettuate per valutare la resistenza a corrosione di leghe di magnesio anodizzate.

INTRODUCTION

Magnesium alloys are the lightest among the structural metals and despite their low density they are still not widely used because of low corrosion resistance even though nowadays the magnesium alloys, containing controlled amounts of iron, copper and nickel, are inherently more corrosion resistant. A surface treatment for protection against general and galvanic corrosion is usually required in case of aggressive environments. Several surface finishing techniques are available to improve corrosion resistance, such as chemical conversion, electrodeposition, physical vapour deposition, chemical vapour deposition, thermal spray, painting and anodic oxidation [1].

Among the surface treatments, high voltage anodic oxidation in micro-arc regime (MAO) is one of the most investigated for

magnesium alloys. By means of this process a porous oxide layer is formed, which significantly modifies the surface properties and favours the adhesion of post-treatment coatings, for example painting [2]. In the anodic oxidation at high voltage, an intense sparking occurs at the magnesium surface when its voltage is greater than breakdown voltage U_B [3].

According to Ikonopisov [4], U_B depends on anodizing solution electrical conductivity k and alloy composition ($U_B = a - b \log k$, a and b parameters dependent on the specific alloy). The oxidation process is related to three different phenomena [5]. At the beginning, during the initial cell voltage ramp, electrolysis of water occurs and a thin insulating film (MgO) is generated on the surface of the magnesium alloy (phenomenon 1). With the increase of

the cell voltage, the MgO dielectric film breakdown occurs and sparks, appearing at the interface electrolyte/anode, rapidly move on the surface and quickly are extinguished; as a consequence, the film becomes porous (phenomenon 2). The breakdown is associated with the tensile stresses in the barrier film that has a molar volume smaller than the metal from which it is formed. When the voltage is further increased, larger sparks remain steadily on the surface and the porosity increases further (phenomenon 3). The three layers have different morphologies: the first layer is semi-transparent, the second has a large number of micro-pores and the third has a large number of big pores [6]. Such porosity does not guarantee a good corrosion protection although it can be a good adhesion interlayer between the

magnesium and a substrate and ceramic or organic post-treatment coatings [7].

In the present paper the influence of electrolyte composition on the morphology and corrosion resistance of anodic oxide was investigated.

EXPERIMENTALS

Anodic oxidation experiments were performed on a die cast AM60B alloy (Q-panel) provided by Norsk Hydro (Table 1). Specimens of 10 cm x 1.5 cm (thickness 0.3 cm) were cut from Q-panels, anodized on both faces in a strongly alkaline solution (Table 2) prepared from ACS grade reagents and by using a Pyrex cell (250 cm³). Two AISI 316 panels were used as cathodes. The anodization bath composition was taken from a paper of Hsiao [8]. The operating conditions were optimized in a previous research [9].

The distance between the magnesium specimen and the cathodes was about 3-4 cm. The anodic oxidation was performed with the electrolytic solution initially at room temperature, and by increasing the cell voltage up to 70 V (maintenance voltage) in 4 min, and by maintaining that value for 6-11 min (total time 10-15 min). During the initial cell voltage ramp, gas evolution at the electrodes was observed. Beyond a threshold cell voltage (around 55 V), sparking occurred randomly on the surface anode. The sparks are initially small and fleeting, while at higher cell voltage,

they become more intense and occur over the whole surface of the anode. In the last minutes, sparking is progressively less intense until it disappears.

After the anodization treatment the surface morphology and the elemental composition were evaluated by scanning electron microscopy (SEM) and x-ray photoelectron spectroscopy (XPS). The phase composition of the anodic oxide layer was assessed by x-ray diffraction (XRD) respectively. The electrochemical polarization tests permit to estimate the corrosion current density (I_{corr}) and the corresponding corrosion potential value (E_{corr}). The measurements of the untreated and anodized specimens were conducted in aqueous solutions of NaCl 3.5% w/w at 25°C, at a scan rate of 5 mV s⁻¹. A conventional three electrode cell was used for the polarization measurements: a platinum mesh was used as counter electrode, a saturated calomel electrode (SCE) as the reference electrode.

RESULTS AND DISCUSSION

Fluoride is considered a harmful species and efforts are done in order to avoid, when possible, its use in surface finishing processes.

Several anodic oxidation experiments were carried out by using a fluoride free solution (Table 3) at three different voltages, 70, 80, and 90 V, and the morphology and corrosion resistance behaviour of the film was evaluated.

As it is shown in the micrograph of Figure 1, referring to the sample obtained at 70 V, the surface is covered by an uneven thin film: the breakdown voltage of β -phase ($Al_{12}Mg_{17}$) is higher than that of α -phase, and as a consequence the β -phase is left uncovered (network on the sample surface in Figure 1).[10]

During the anodization at 80 V, sparks randomly move on the surface and the

Table 1. Chemical composition of AM60B alloy (wt. %)

Al	Zn	Mn	Si	Fe	Cu	Ni	Mg
5.9	0.05	0.27	0.025	0.0017	0.0017	0.0004	balance

Table 2. Composition of the optimized anodizing solution and operating conditions

Electrolyte	Concentration (mol dm ⁻³)		Operating conditions	
	KOH	Na ₃ PO ₄ ·12H ₂ O	Cell voltage [V]	Time [min]
KOH	3.0		70	15
Na ₃ PO ₄ ·12H ₂ O	0.21			
KF	0.6			
Al(NO ₃) ₃ ·9H ₂ O	0.15			

Table 3. Effect of KF concentration on MAO of AM60B

KOH	Na ₃ PO ₄ ·12H ₂ O	Concentration (mol dm ⁻³)		Operating conditions	
		KF	Al(NO ₃) ₃ ·9H ₂ O	Cell voltage [V]	Time [min]
3.0	0.21	-	0.15	70	15
				80	
				90	

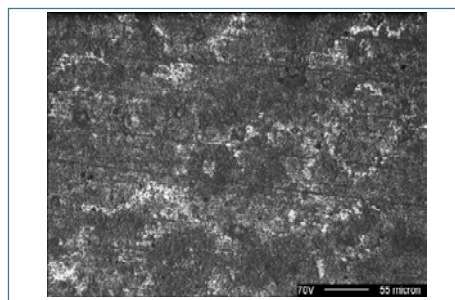


Fig. 1: Optical micrograph of the surface of a sample anodized at 70 V (15 min, fluoride free solution).

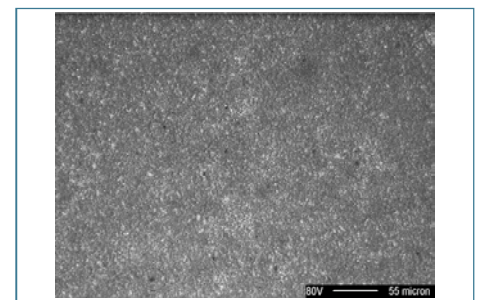


Fig. 2: Optical micrograph of the surface of a sample anodized at 80 V (15 min, fluoride free solution).

resulting oxide is porous (Figure 2), with greater porosity where the sparks were more persistent. A visual examination of the anodic oxide produced at 90 V shows several localized attacks of the surface due to sparking. Electrochemical polarization tests performed on the sample produced at 80 V show that the anodized sample in a fluoride free solution has more negative potential (about 100 mV) in comparison with the sample obtained in a fluoride containing solution, probably due to the formation of an insoluble film of MgF_2 (Figure 3).

Visual examination, optical microscope analysis and electrochemical polarization tests allow to resolve that it is possible to anodize magnesium alloys in free fluoride solutions and achieving similar properties in respect to the samples anodized in fluoride containing solutions by slightly increasing the cell voltage.

The influence of other electrolytes was investigated. Table 4 lists the experimental conditions adopted to evaluate the effect of *potassium hydroxide* on the breakdown voltage and the oxide morphology. For each concentration of KOH three different cell voltages were tested (75, 80, 85 V).

For KOH concentrations lower than 3 mol dm^{-3} (in particular 2.5 and 2.0 mol dm^{-3}) anodic oxides have a non uniform appearance (Figure 4). Moreover, in test 4, an intense gas evolution occurred, accompanied by quick increase (up to 80°C) of anodizing solution temperature and localized attacks of the AM60B alloy. The oxide layer shows severe attacks due to the corrosion of magnesium alloy in strongly alkaline media at high temperature (greater than 60°C), consequently it is impossible to decrease KOH concentration without impairing of the oxide quality (Figure 4).

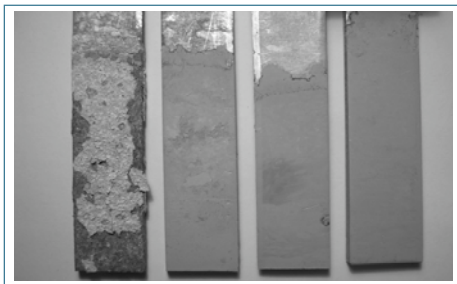


Fig. 4: Effect of KOH concentration on AM60B micro-arc anodic oxidation (from left: 1.0, 2.0, 2.5, 3.0 mol dm^{-3}).

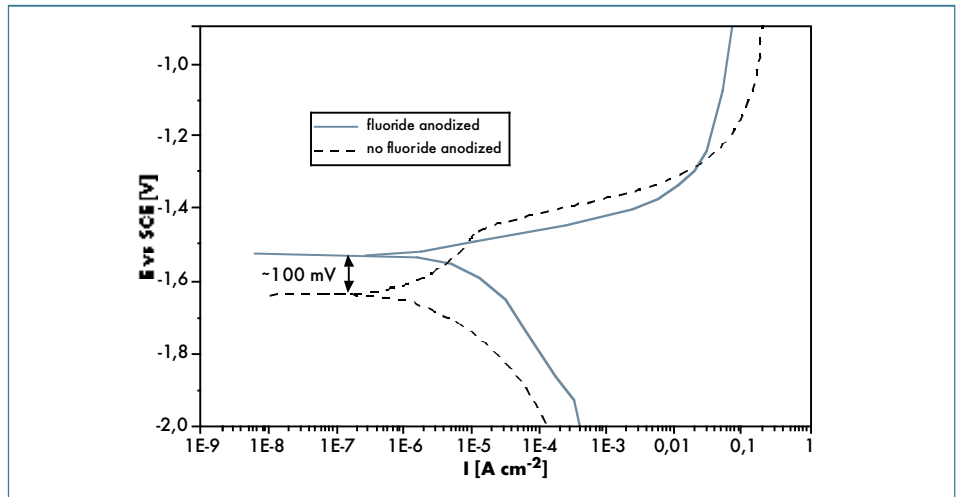


Fig. 3: Electrochemical polarization curves for anodized AM60B samples (dashed line: no fluoride, continuous line: fluoride) at 25°C , scan rate 5 mV s^{-1} in $\text{NaCl } 3.5\% \text{ w/w}$.

Table 4. Effect of KOH concentration on MAO of AM60B

Test	Concentration (mol dm^{-3})			Operating conditions	
	KOH	$\text{Na}_3\text{PO}_4 \cdot 12\text{H}_2\text{O}$	$\text{Al}(\text{NO}_3)_3 \cdot 9\text{H}_2\text{O}$	Cell voltage [V]	Time [min]
1	3.0	0.21		75	
2	2.5	0.21		80	15
3	2.0	0.21	0.15	85	
4	1.0	0.21			

To evaluate the influence of KOH concentration on the breakdown voltage eight samples were anodized in more concentrated solution (from 2 up to about 20 mol dm^{-3} , saturated solution at 20°C). By increasing the KOH concentration the breakdown voltage drops in exponential

way (Figure 5) and the oxide thickness progressively decreases. This fact can be attributed to the predominant oxide dissolution compared to its growth.

The influence of sodium phosphate on the anodization process was evaluated by performing a large number of tests, as

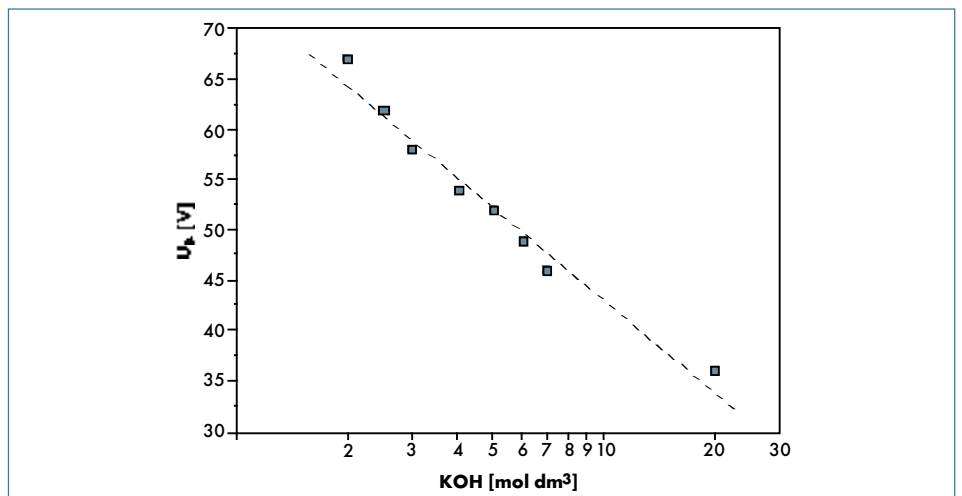


Fig. 5: Breakdown voltage vs KOH concentration.

Table 5. Effect of Na_3PO_4 concentration on MAO of AM60B

Test	Concentration (mol dm ⁻³)			Operating conditions	
	KOH	$\text{Na}_3\text{PO}_4 \cdot 12\text{H}_2\text{O}$	$\text{Al}(\text{NO}_3)_3 \cdot 9\text{H}_2\text{O}$	Cell voltage [V]	Time [min]
1		0.00			
2		0.05			
3		0.10		75	
4	3	0.15	0.15	80	15
5		0.21		85	
6		0.25			
7		0.30			

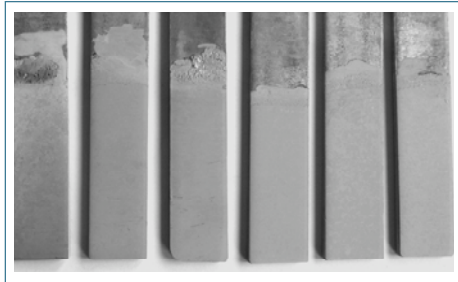


Fig. 6: Effect of Na_3PO_4 concentration on AM60B micro-arc anodic oxidation at 80 V (from left: 0.05, 0.10, 0.15, 0.21, 0.25, 0.30 mol dm⁻³).

When sodium phosphate concentration is lower than 0.21 mol dm⁻³ the anodic oxide is not uniform. On the other hand, in the range 0.21-0.25 mol dm⁻³ it is even and homogeneous; beyond 0.25 mol dm⁻³ the sparks become very intense and persisting in some preferential spots of the surface, causing severe attack. Therefore, phosphates are fundamental to guarantee a uniform layer as they favour uniform sparking distribution on the sample surface. In order to obtain even oxides at high phosphate concentration the cell voltage must be decreased. As shown in Figure 7 the breakdown potential linearly decreases by increasing the phosphate concentration. Electrochemical polarizations tests (Figure 8) were performed on the most homogeneous samples, obtained at different voltages and different phosphate concentrations. As shown in Figure 8, there are not significant differences in the corrosion current densities among the anodized samples, whereas the corrosion current density of the base AM60B is two orders of magnitude higher.

To evaluate the aluminium nitrate influence on the anodic oxide morphology and corrosion resistance, some samples were anodized in solutions containing different aluminium nitrate concentrations (Table 6).

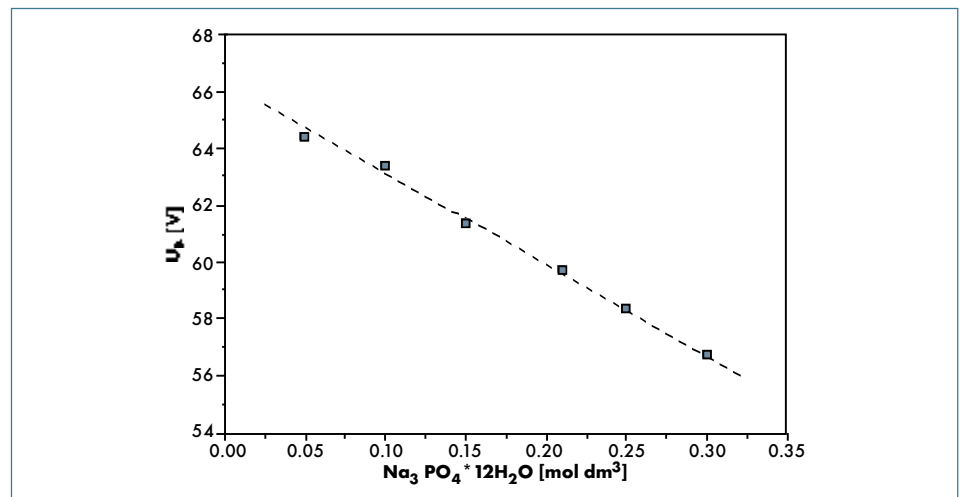


Fig. 7: U_B (V) vs $\text{Na}_3\text{PO}_4 \cdot 12\text{H}_2\text{O}$ concentration.

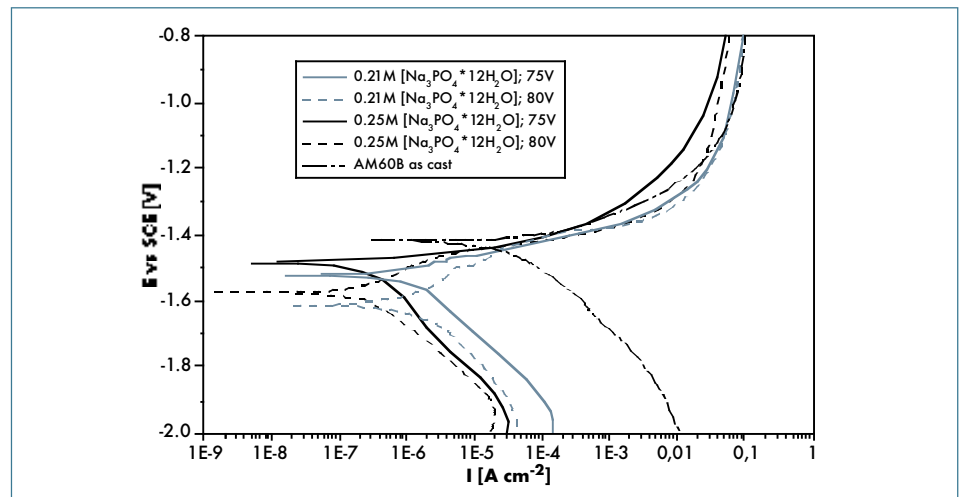


Fig. 8: Electrochemical polarizations tests (NaCl 3.5% w/w, 25°C 5mV s⁻¹).

Tests performed at 80 V with aluminium nitrate concentration 0.21 and 0.25 mol dm⁻³ were interrupted because of intense gas evolution and heat release, then tests were carried out at 75 V. Electrical

conductivity at room temperature of test solution 1 was 175 mS cm⁻¹ and sparking occurred at 50 V, while in the case of test solution 6 conductivity was 148 mS cm⁻¹ and sparking occurred at 64 V. These

Table 6. Effect of $\text{Al}(\text{NO}_3)_3 \cdot 9\text{H}_2\text{O}$ concentration on MAO of AM60B

Test	Concentration (mol dm^{-3})			Operating conditions	
	KOH	$\text{Na}_3\text{PO}_4 \cdot 12\text{H}_2\text{O}$	$\text{Al}(\text{NO}_3)_3 \cdot 9\text{H}_2\text{O}$	Cell voltage [V]	Time [min]
1			0.00		
2			0.05		
3	3	0.21	0.10	75	15
4			0.15	80	
5			0.20		
6			0.25		

results are in agreement with findings of Khasalev [11] and Hsiao [12]. From our results, in disagreement with Hsiao [12] it seems that the absence of $\text{Al}(\text{NO}_3)_3$ does not affect spark distribution, which seems to be mostly controlled by sodium phosphate. In the range 0.15-0.21 mol dm^{-3} anodic oxides are more uniform and thicker than those obtained at lower concentrations of aluminium nitrate. At higher concentrations sparking was excessive and caused localized attack. Experimental results agree with findings of Khasalev [10], the oxide thickness increases with aluminium nitrate concentration increasing. Electrochemical polarization tests resulted in lower corrosion current densities for aluminium nitrate concentration of 0.25 mol dm^{-3} , in agreement with Hsiao et al. [8, 12]. Lower and higher concentrations of $\text{Al}(\text{NO}_3)_3$ caused unacceptable corrosion resistance due respectively to the small thickness and the great porosity of the oxide. Figure 9 shows polarization curves at different aluminium nitrate concentrations at 75 V.

In order to optimize process times, some tests were performed at different anodizing times, in the range from 10 min to 60 min at 80 V in the solution of Table 3. Anodic oxides obtained in anodizing times of 10, 15, 30 and 45 min have similar thicknesses, ranging between 1.2 and 1.7 μm . After 60 min, oxide thickness was 0.45 μm , probably because the oxide dissolution is predominant compared to growth for longer times. Thereby 10 min of anodizing time is considered the best compromise time – thickness. Figure 10 shows the SEM surface morphology and fracture of the anodic oxide obtained at 80 V in 10 minutes and 60 minutes of anodization, respectively. Anodic oxides are very porous and cracked.

Anodic oxide obtained in KOH 3M, $\text{Na}_3\text{PO}_4 \cdot 12\text{H}_2\text{O}$ 0.21M, $\text{Al}(\text{NO}_3)_3 \cdot 9\text{H}_2\text{O}$ 0.15M, at 80 V for 10 min, was analyzed by EDS and by XRD (Figure 12, Figure 13).

Figure 12 shows the energy dispersive spectroscopy (EDS) spectrum that reveals the presence of oxygen, phosphorus and potassium besides magnesium and aluminium. The x-ray diffraction (XRD) analysis (Figure 13) shows that the anodic oxide mainly consists of magnesium oxide MgO and small amount of phosphate compounds.

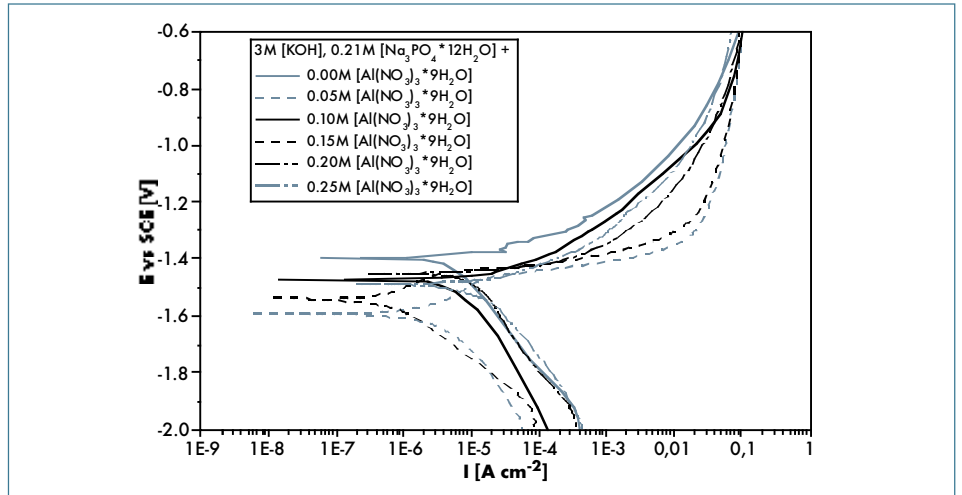


Fig. 9: Electrochemical polarizations curves at different aluminium nitrate concentrations (NaCl 3.5% w/w, 25°C 5mV s^{-1}).

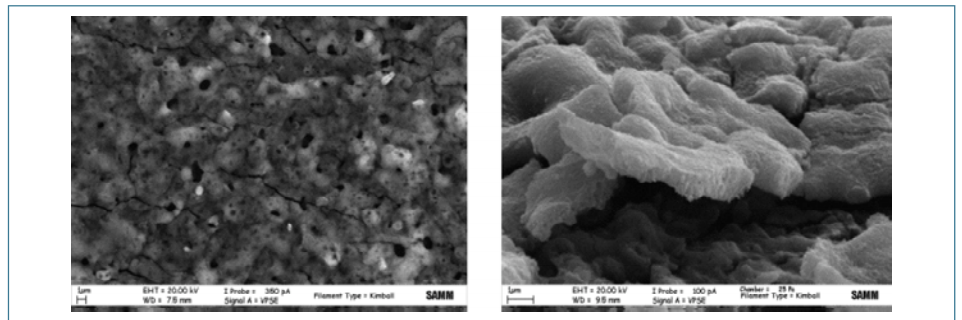


Fig. 10: SEM surface morphology and fracture of anodic oxides (anodizing time: 10 min).

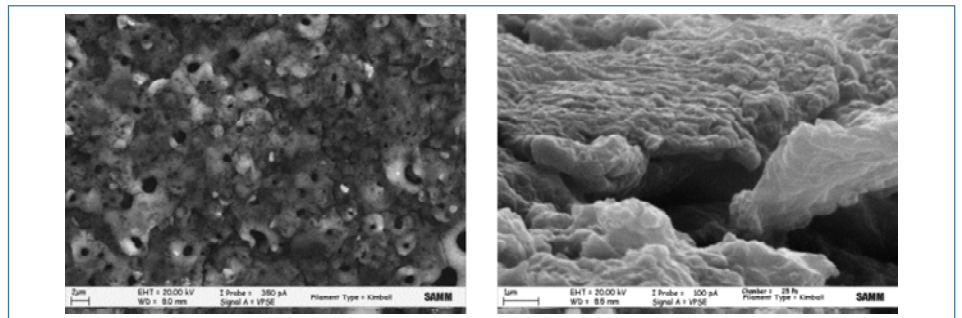


Fig. 11: SEM surface morphology and fracture of anodic oxides (anodizing time: 60 min).

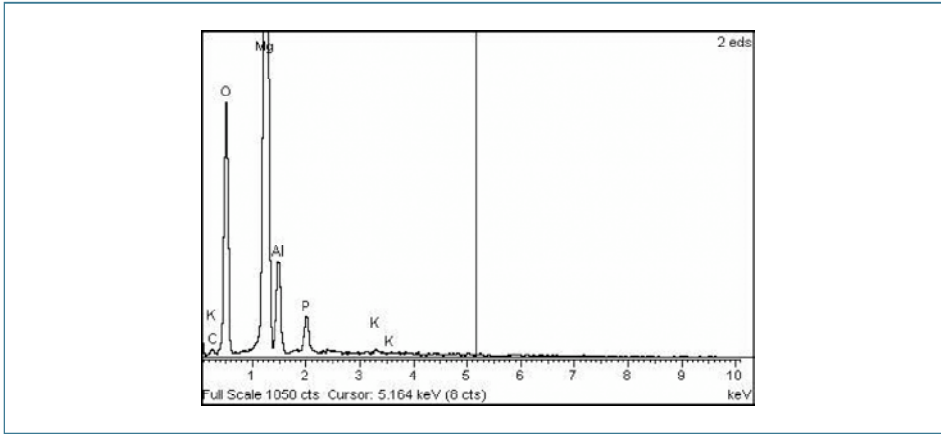


Fig. 12: EDS spectrum of anodic oxide (test 1, table 7).

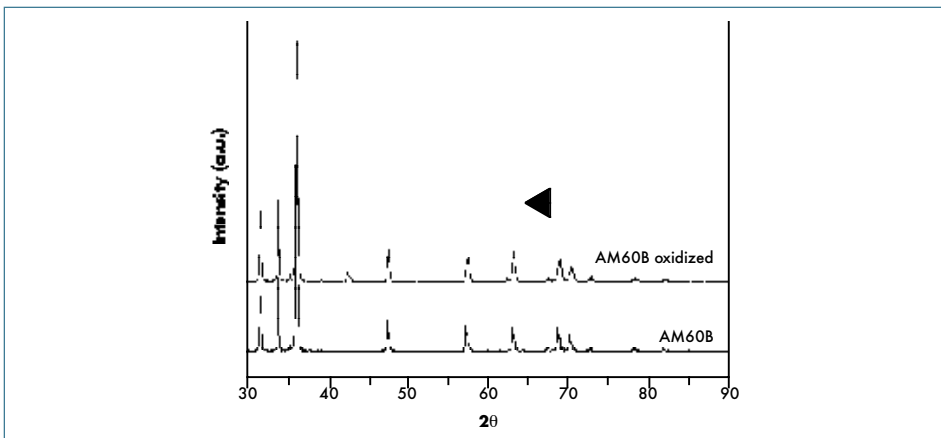


Fig. 13: XRD pattern of anodic oxide (test 1, table 7).

Table 7. Atomic concentration of the elements at different depths

Depth (Å)	%C	%O	%F	%Mg	%Al	%Si	%P	%Ar
0	48.30	37.48	1.31	7.21	4.21	0.91	0.59	0.00
100	9.13	46.62	1.47	29.98	8.34	0.50	0.99	2.97
500	2.44	45.84	1.32	40.17	6.52	0.36	0.31	3.04
1000	2.60	45.01	1.44	41.35	6.21	0.00	0.50	2.89
1500	2.37	44.73	1.46	42.45	5.62	0.00	0.47	2.90
2000	2.09	44.39	1.72	42.87	5.57	0.00	0.49	2.87

Table 8. Anodizing processes

Test	Concentration (mol dm ⁻³)			Operating conditions	
	KOH	Na ₃ PO ₄ ·12H ₂ O	Al(NO ₃) ₃ ·9H ₂ O	Cell voltage [V]	Time [min]
1		0.21		80	
2	3	0.25	0.15	75	15
3		0.25		80	

Table 7 reports the atomic concentration of the elements measured by x-ray photoelectron spectroscopy (XPS), at different depths, below the surface of an anodic oxide obtained with operating conditions related in Table 2. The comparison between Mg and Al measured atomic concentration values and the theoretical ones (Mg 46.58 %, Al 2.64%) reveals a significant surface enrichment in aluminium. This result can be ascribed to the MAO process. In fact, sparks are associated to heat release and magnesium and alloying elements are locally melted out of the substrate. Afterwards, they enter the discharge channel and got anodized, electrolyte can enter and be trapped in the oxide. These phenomena explain the presence of fluorine and phosphorus in the coating, not present in the base alloy.

Surface morphology and fracture surfaces of anodized samples are displayed in Figure 14.

The oxide obtained in test 1 presents smaller pores than those obtained in tests 2 and 3. This is attributed to a less intense sparking activity during anodic oxidation,

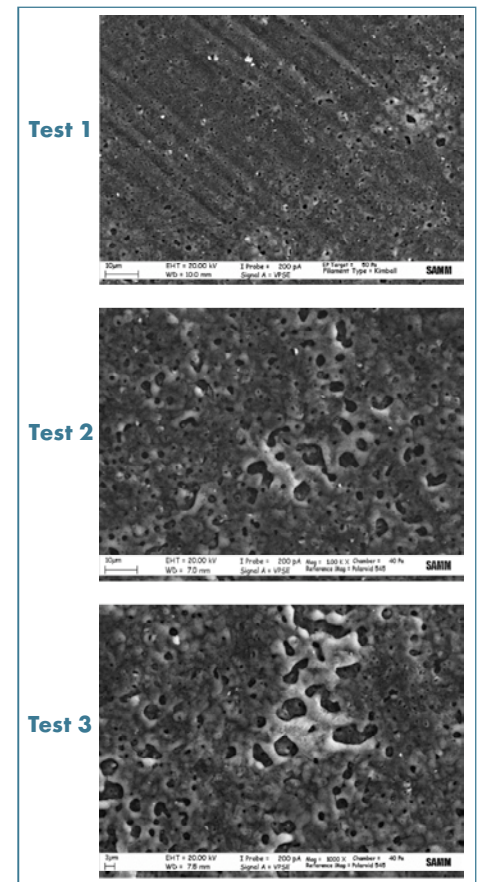


Fig. 14: SEM surface morphology of the anodized samples.

Table 9. Thickness, roughness and micro hardness of anodic oxides

Sample	Oxide thickness	Roughness - Ra [μm]	Hardness [HV]
1	1.6	0.530	181±18
2	2.7	0.417	149±25
3	4.7	0.444	302±62
Fluoride	1.4	0.318	170±23
AM60B	-	-	120±27

however producing a thinner layer (Table 9). The anodized sample in fluoride solution (Table 2) presents a decreased roughness, Vickers microhardness and thickness than those produced in fluoride free solution, in agreement with Barton and Johnson [13]. Micro-hardness measurements (10 mN for 10 sec) show lower values for test 2 than for tests 1 and 3. This can be related to lower internal stresses generated in the oxide at lower potentials (75 vs 80 V). Potentiodynamic curves of anodized samples (Table 8), fluoride anodized samples (Table 2) and as cast AM60B alloy are reported in Figure 15.

E_{corr} of anodized samples is slightly lower (-1.46 ÷ -1.62 V vs SCE) than the value of the as cast AM60B alloy (-1.42 V vs SCE). I_{corr} of anodized samples is two orders of magnitude lower than AM60B ($5 \cdot 10^{-5} \text{ A cm}^{-2}$). In particular, the samples produced according the parameters of Table 8 produce corrosion current densities an order of magnitude lower ($3 \cdot 10^{-7} \div 2 \cdot 10^{-7} \text{ A cm}^{-2}$) than those observed for the process of Table 2 ($2 \cdot 10^{-6} \text{ A cm}^{-2}$). This result may be explained with the increased barrier effect of the thicker oxides.

CONCLUSIONS

The influence of electrolyte composition on the morphology and corrosion properties of the anodic oxide produced by MAO on AM60B alloy was investigated. Decreasing or increasing the potassium hydroxide concentration with respect to the optimum value of 3M gave poor quality oxides. The use of fluorides could be avoided by a slight increase of the anodizing voltage, although roughness was also slightly increased. Phosphate is a fundamental constituent to achieve a uniform distribution of sparks on the whole surface area and to avoid fixed sparks and consequent macroporosity. Aluminium nitrate is fundamental to obtain an oxide layer with good protection properties against corrosion. The anodic layer mainly consists of MgO, with small amount of aluminium oxide and/or other phosphate compounds. Electrochemical polarization tests highlight that anodic oxides corrosion currents are two orders of magnitude lower than those of as cast magnesium alloys. The anodic oxide produced in MAO regime on AM60B alloy can be used as an intermediate layer for post-treatment finishing (e.g., painting, sol-gel, electrophoretic treatments).

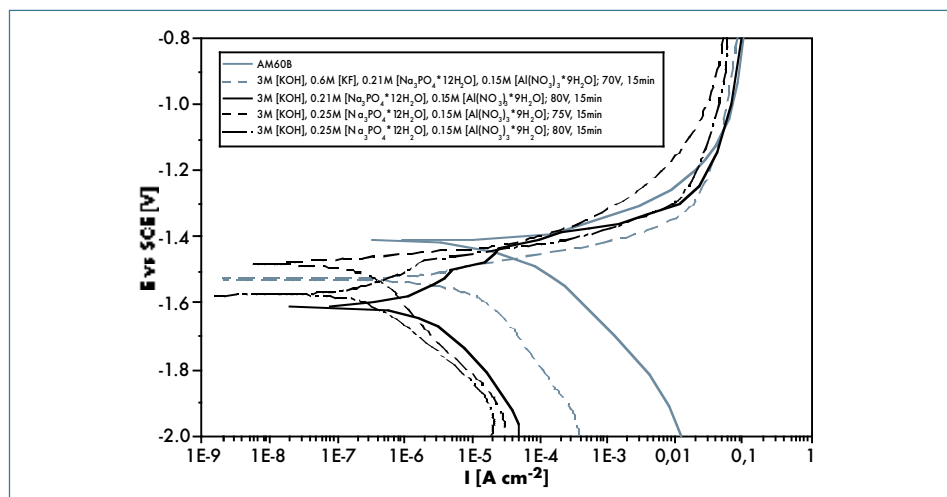


Fig. 15: Electrochemical polarization curves (25°C, NaCl 3.5%, 5mV s⁻¹).

ACKNOWLEDGEMENTS

Aknowledgements are due to Fondazione Cariplo for financial support of the project "Penetrazione industriale delle leghe di magnesio", Grant No. 2003.1891/10.4877.

REFERENCES

- [1] Gray J.E and B.Luan. Protective coatings on magnesium and its alloys- a critical review. *Journal of Alloys and Compounds*, 336 (2002), 88-113.
- [2] Bestetti M., P.L. Cavallotti, A. Da Forno and S. Pozzi. Anodic oxidation and powder coating for corrosion protection of AM60B magnesium alloys. *Transactions of the Institute of Metal Finishing*, 85(6) (2007), 316-319.
- [3] Blawert C., W. Dietzel, E. Ghali and G. Song. Anodizing Treatments for Magnesium Alloys and Their Effect on Corrosion Resistance in Various Environments. *Advanced Engineering Materials*, 8(6) (2006), 511-533.
- [4] Ikonopisov S. Theory of electrical breakdown during formation of barrier anodic films. *Electrochimica Acta* 22 (1977), 1077-1082.
- [5] Verdier S., M. Boinet, S. Maximovitch and F. Dalard. Formation, structure and composition of anodic films on AM60B magnesium alloy obtained by DC plasma anodising. *Corrosion science*, 47(2005), 1429-1444.
- [6] Wang Y., J. Wang, J. Zhang and Z. Zhang. Effect of spark discharge on the anodic coatings on magnesium alloy. *Materials Letters*, 60 (2006), 474-478.
- [7] Guglielmi M. Sol-Gel Coatings on Metal. *Journal of Sol-Gel Science and Technology*, 8 (1997) 443-449.
- [8] Hsiao H-Y. and W-T. Tsai, Characterization of anodic films formed on AZ91D magnesium alloy. *Surface & Coatings Technology*, 190 (2005), 299-308.
- [9] Pozzi S. Ossidazione anodica di leghe di magnesio in funzione prevemiciatura. *Tesi* (2007).
- [10] Khasalev O., D. Weiss, and J. Yahalom, Structure and composition of anodic films formed on binary Mg-Al alloys in KOH-aluminate solutions under continuous sparking. *Corrosion science*, 43 (2001), 1295-1307.
- [11] Khasalev O. and J. Yahalom, The anodic behaviour of binary Mg-Al Mg alloys in KOH-aluminate solutions. *corrosion Science*, 40(7) (1998), 1149-1160.
- [12] Hsiao H. , H. Tsung and W. Tsai, Anodization of AZ91D magnesium alloy in silicate-containing electrolytes. *Surface & Coatings Technology*, 199 (2005), 127-134.
- [13] Barton T.F. and C.B. Johnson . The effect of electrolyte on the anodized finish of a magnesium Alloy. *Plating & Surface Finishing*, May (1995), 138-141.